

# MicroRNA-detargeting proves more effective than *leader* gene deletion for improving safety of oncolytic Mengovirus in a nude mouse model

Yogesh R. Suryawanshi,<sup>1</sup> Rebecca A. Nace,<sup>1</sup> Stephen J. Russell,<sup>1,2</sup> and Autumn J. Schulze<sup>1</sup>

<sup>1</sup>Department of Molecular Medicine, Mayo Clinic College of Medicine, 200 1<sup>st</sup> Street S.W., Rochester, MN 55905, USA; <sup>2</sup>Division of Hematology, Mayo Clinic, Rochester, MN 55905, USA

**A dual microRNA-detargeted oncolytic Mengovirus, vMC<sub>24</sub>NC, proved highly effective against a murine plasmacytoma in an immunocompetent syngeneic mouse model; however, there remains the concern of escape mutant development and the potential for toxicity in severely immunocompromised cancer patients when it is used as an oncolytic virus. Therefore, we sought to compare the safety and efficacy profiles of an attenuated Mengovirus containing a virulence gene deletion versus vMC<sub>24</sub>NC in an immunodeficient xenograft mouse model of human glioblastoma. A Mengovirus construct, vMC<sub>24</sub>ΔL, wherein the gene coding for the leader protein, a virulence factor, was deleted, was used for comparison. The vMC<sub>24</sub>ΔL induced significant levels of toxicity following treatment of subcutaneous human glioblastoma (U87-MG) xenografts as well as when injected intracranially in athymic nude mice, reducing the overall survival. The *in vivo* toxicity of vMC<sub>24</sub>ΔL was associated with viral replication in nervous and cardiac tissue. In contrast, microRNA-detargeted vMC<sub>24</sub>NC demonstrated excellent efficacy against U87-MG subcutaneous xenografts and improved overall survival significantly compared to that of control mice without toxicity. These results reinforce microRNA-detargeting as an effective strategy for ameliorating unwanted toxicities of oncolytic picornaviruses and substantiate vMC<sub>24</sub>NC as an ideal candidate for clinical development against certain cancers in both immunocompetent and immunodeficient hosts.**

## INTRODUCTION

MicroRNAs (miRNAs) are small non-coding RNAs that function as post-transcriptional gene regulators by targeting mRNAs for translational repression or enzymatic degradation. Although a variety of miRNAs are universally expressed, many have distinct cell/tissue type-specific signatures. Additionally, these specific patterns of expression are often dysregulated in cancer cells.<sup>1</sup> Furthermore, insertion of sequences targeted by these cell type-specific miRNAs into foreign genetic material, such as gene therapies or oncolytic viruses, can effectively repress foreign gene expression in a cell type-specific manner, a phenomenon known as miRNA-detargeting. Owing to this, miRNA-detargeting has become an effective method for selectively controlling the tissue tropism and toxicity of a variety of RNA and DNA viruses.<sup>1–14</sup> Our laboratory has previously demon-

strated that the miRNA-detargeting strategy can be used to moderate the neuro- and cardiotoxicities associated with a poly(C) truncated oncolytic Mengovirus, vMC<sub>24</sub>, while retaining the virus' ability to replicate in a wide range of murine and human cancer cells.<sup>12</sup> This virus, vMC<sub>24</sub>NC, generated by inserting neuron- and cardiac/muscle-specific miRNA targets into the 5' and 3' non-coding regions (NCRs) of the viral genome, showed excellent therapeutic efficacy against a syngeneic murine plasmacytoma (MPC-11) model without significant virus-mediated toxicity. Despite the success of miRNA-detargeting in controlling pathogenesis of a variety of oncolytic viruses, particularly picornaviruses, development of escape mutants and possible reversion to a virulent phenotype remains a concern with little to no clinical data.<sup>1–14</sup> Although virus escape from miRNA-mediated inhibition may be less of a concern in immunocompetent hosts, as the virus can be cleared prior to evolution, the safety of these viruses in immunocompromised hosts needs to be thoroughly analyzed.

New therapeutics are desperately needed for treating glioblastoma multiforme (GBM) because of a low overall survival among these patients with standard cancer therapeutics.<sup>15–17</sup> Oncolytic viruses have emerged as a prime candidate for treatment of GBM and other cancers, as these viruses have the potential to break immune tolerance within the highly immunosuppressive tumor microenvironment (TME) of GBM tumors and boost response to immunotherapies that could otherwise have a suboptimal efficacy by themselves.<sup>18–20</sup> A wide range of oncolytic viruses are being tested in GBM patients in various phases of clinical trial, including picornaviruses.<sup>21,22</sup> Picornaviruses present as desirable candidates to be developed as oncolytic agents because of their unique biological attributes, such as the small size of the capsid that facilitates penetration of the blood-brain barrier, which is one of the major hurdles in treating GBM tumors. Our previous study demonstrated that Mengovirus has the ability to reach the brain when injected systemically.<sup>12</sup> Among the oncolytic

Received 19 March 2021; accepted 19 August 2021;  
<https://doi.org/10.1016/j.omto.2021.08.011>

**Correspondence:** Autumn J. Schulze, PhD, Department of Molecular Medicine, Mayo Clinic College of Medicine, 200 1<sup>st</sup> Street S.W., Rochester, MN 55905, USA.  
**E-mail:** [schulze.autumn@mayo.edu](mailto:schulze.autumn@mayo.edu)



picornaviruses, a polio:rhinovirus chimera (PVSRIPO) is the most well-studied virus that has reached the level of clinical trial for the treatment of GBM (NCT01491893, NCT03043391), while other members of the *Picornaviridae* family are still at a pre-clinical phase.<sup>23</sup> Oncolytic Seneca Valley virus (SVV) has been investigated in two phase I and one phase II clinical trials. SVV was well tolerated in a phase I trial, either as a monotherapy or in combination with cyclophosphamide, in pediatric patients with relapsed/refractory solid tumors including neuroblastomas.<sup>24</sup> In another phase I study, SVV was also well tolerated in patients with small cell lung carcinoma with neuroendocrine features and showed replication in tumors.<sup>25</sup> These results prompted its promotion to phase II investigation; however, it failed to significantly improve progression-free survival.<sup>26</sup>

Mengovirus, a member of the *Picornaviridae* family, has several desirable features as an oncolytic virus, such as a broad host and tissue tropism,<sup>27</sup> low seroprevalence in the human population,<sup>28</sup> and evidence of successful use as a vaccine candidate against encephalomyocarditis virus (EMCV), a serologically related cardiovirus, that warrant the development of Mengovirus as an oncolytic agent.<sup>29–31</sup> It has been reported that nervous tissue-specific miRNA miR-124 is downregulated both in a panel of different grades of glioma tissues and in human glioma cell lines.<sup>32</sup> This could allow selective replication of vMC<sub>24</sub>NC in GBM cells, enhancing therapeutic efficacy while circumventing the virus-mediated neurotoxicity, because this virus is engineered to be detargeted from tissues expressing high levels of miR-124. Previous studies from our lab have shown that Mengovirus can be effectively detargeted from nervous and cardiac tissue via miRNA-detargeting to eliminate virus toxicity without losing efficacy, but there remains the concern that the miRNA response elements can develop mutations or be completely deleted under selective pressure.<sup>12</sup> This can potentially lead to reversion of the Mengovirus to its parental form and cause toxicity *in vivo*, particularly in severely immunocompromised hosts, such as GBM patients. This prompted us to evaluate the rate of vMC<sub>24</sub>NC escape as well as to look into alternative ways of attenuating Mengovirus toxicity while retaining its efficacy in cancer cells for comparative analysis in an immunocompromised mouse model of GBM.

One way to attenuate Mengovirus is via deletion of its virulence genes, such as the *leader* gene, which encodes for the leader protein that allows successful viral replication by antagonizing apoptosis,<sup>33</sup> blocking the interferon (IFN) response,<sup>34</sup> and preventing induction of the stress response in infected host cells.<sup>35</sup> Deletion of the *leader* gene attenuates Mengovirus and has been shown to eliminate viral toxicity when injected intracranially (i.c.) in immunocompetent mice.<sup>34</sup> Unlike miRNA-detargeted vMC<sub>24</sub>NC, the *leader*-knockout Mengovirus would not be vulnerable to point or deletion mutations that could lead to reversion of the virus to a toxic parental strain. Patients with GBM are immunosuppressed because of the cancer itself and chemo/radiotherapy, which makes the safety of oncolytic viruses to be used in these patients of the utmost importance. In this study, we assessed the safety of vMC<sub>24</sub>ΔL, a poly(C) truncated Mengovirus with the *leader* gene deletion, and vMC<sub>24</sub>NC in an athymic nude

mouse model that is known to have a compromised immune system due to T lymphocyte dysfunction.<sup>36</sup> Testing the safety of these viruses in an athymic nude mouse model in the presence and absence of subcutaneous GBM tumors provided a clinically relevant analysis of the safety of these viruses in immunocompromised individuals such as GBM patients. Notably, injection of vMC<sub>24</sub>ΔL both i.c. and intratumorally (i.t.) in mice bearing human glioblastoma xenografts resulted in significant toxicity, contrary to vMC<sub>24</sub>NC, which showed potent efficacy with minimal toxicity. Mutations in the miRNA response elements of vMC<sub>24</sub>NC were observed at a relatively earlier stage post-treatment in immunodeficient athymic nude mice than our previous studies in an immunocompetent syngeneic plasmacytoma mouse model.<sup>12</sup> This could be due to different levels of viral quasispecies among different virus stocks or due to different selection pressures exerted by the host immune system between immunocompetent and immunodeficient mice.

## RESULTS

### Deletion of the *leader* gene attenuates Mengovirus in a cell type-specific manner compared to vMC<sub>24</sub> and vMC<sub>24</sub>NC

Mengovirus leader protein inhibits the activation of the type I IFN response pathway by inhibiting the transcription of IFN-stimulated genes.<sup>37,38</sup> Deletion of the *leader* gene has been shown to attenuate Mengovirus because of activation of IFN-stimulated genes at the immediate-early stage of infection, inducing an anti-viral state in host cells and preventing virus spread.<sup>34</sup> Mengovirus with the *leader* gene deletion, vMC<sub>24</sub>ΔL, was generated by deleting bases encoding amino acids 12–52 (Figure 1A) in the leader protein. vMC<sub>24</sub>ΔL replicated, spread, and exhibited cytotoxic effects similar to unmodified vMC<sub>24</sub> and vMC<sub>24</sub>NC in BHK-21 producer cells (Figure 1B). vMC<sub>24</sub>ΔL infection and spread in BHK-21 cells were unrestricted partially because of the defective IFN response pathway in these cells.<sup>39</sup> The enhanced cell killing efficiency of vMC<sub>24</sub>ΔL observed in BHK-21 cells infected with a low MOI of 0.01 at 24 hours post infection (hpi) could be due to activation of caspase-mediated apoptosis, as the leader protein has been shown to impede immediate caspase-mediated apoptosis induction in host cells to promote virus replication.<sup>33,40,41</sup> In contrast to BHK-21 cells, vMC<sub>24</sub>ΔL replication in U87.luc cells was markedly attenuated at both high and low MOI compared to vMC<sub>24</sub> and vMC<sub>24</sub>NC (Figure 1C, top). At high MOI, vMC<sub>24</sub>ΔL induced cell death resulting in observable cell killing by 24 hpi, corresponding with peak, albeit low, virus titers that remained unchanged at 72 hpi (Figure 1C). Although vMC<sub>24</sub>ΔL titer rose slightly over 72 hpi at low MOI in U87.luc cells, peak virus titers remained a log lower than high MOI infection and no loss in cell viability was observed, indicating that the spread of the virus was insufficient to overcome the growth of the uninfected cells.

### Restriction of vMC<sub>24</sub>ΔL replication is cell type specific

We further investigated whether the attenuated replication of vMC<sub>24</sub>ΔL in U87.luc cells is due to the induction of an IFN-mediated anti-viral state or induction of early apoptosis, since the leader protein is known to antagonize both of these processes in infected host cells.<sup>33,34</sup> Earlier studies suggest that U87-MG cells cannot produce

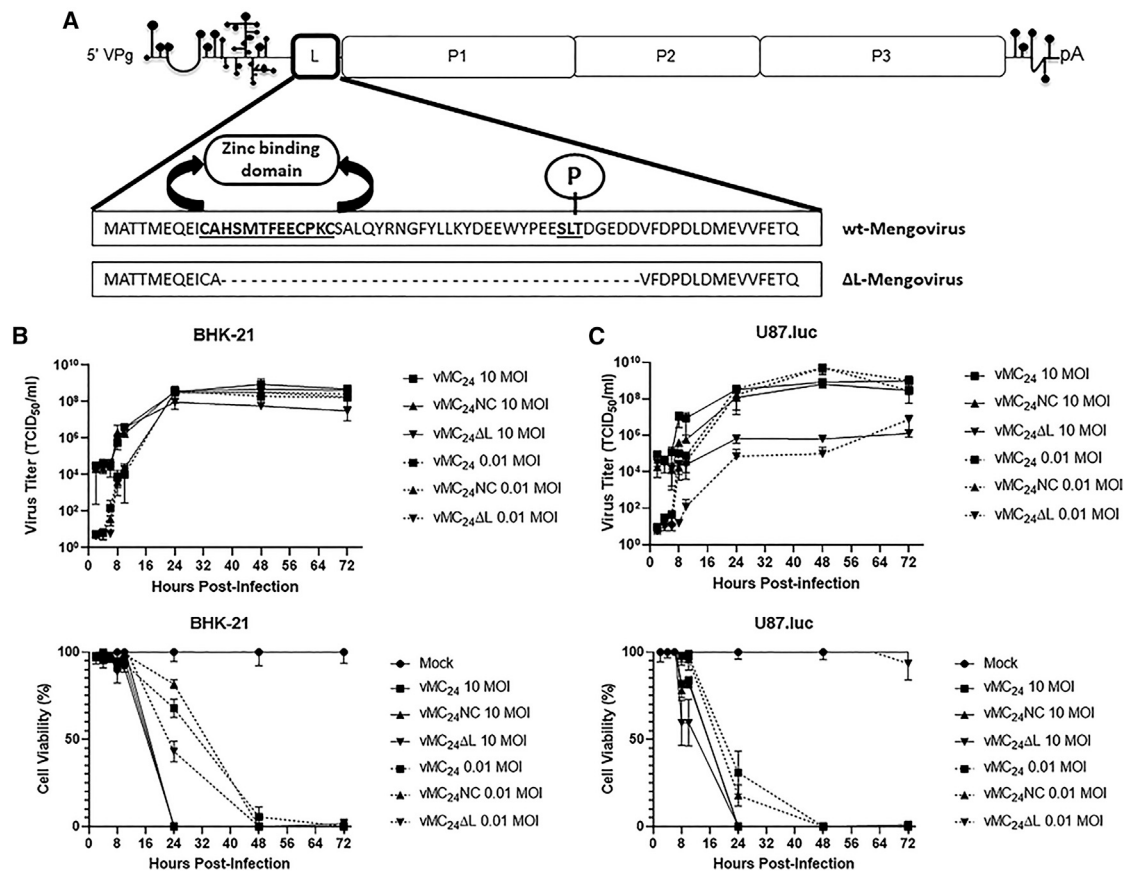


**Figure 1. Generation and characterization of vMC<sub>24</sub>ΔL**

(A) Schematic representation of vMC<sub>24</sub>ΔL showing the Mengovirus genome with the 5' noncoding region (5' NCR), the protein-coding region, the 3' noncoding region (3' NCR), and the poly(A) tail. In the protein coding region *leader* (L) gene encodes the leader protein. The P1 and P2 regions encode the structural and non-structural proteins, respectively. The underlying expanded panel depicts the Leader protein showing the putative zinc-binding domain at the N terminus and the phosphorylation site in the acidic region. Replication kinetics (B and C, top) and cytotoxicity (B and C, bottom) of vMC<sub>24</sub>NC and vMC<sub>24</sub>ΔL were evaluated by single-step and multi-step growth curve analysis (MOI 10, 0.01) and MTT cell viability assay in (B) BHK-21 cells and (C) U87.luc cells. All experiments were repeated at least three times, and data are represented as mean values ± standard deviations.

IFN because of deletion and rearrangement mutations in the IFN gene cluster;<sup>42,43</sup> however, they are responsive to exogenous type I IFN.<sup>44</sup> We verified that U87.luc cells are unable to produce IFN after Mengovirus infection (Y.R.S., unpublished data). Therefore, the restricted replication of vMC<sub>24</sub>ΔL in U87.luc cells was not due to IFN-mediated antagonism in this context. However, IFN- $\alpha$  pretreatment protected the cells from vMC<sub>24</sub>, vMC<sub>24</sub>NC, or vMC<sub>24</sub>ΔL infection at both high and low MOI (Figure S1A), identifying IFN-mediated restriction of replication as a mechanism for attenuation *in vivo*. To this end, we tested the ability of vMC<sub>24</sub>, vMC<sub>24</sub>NC, and vMC<sub>24</sub>ΔL to overcome IFN-mediated resistance in H1HeLa cells that are known to have a responsive IFN pathway after Mengovirus infection.<sup>34</sup> Whereas both vMC<sub>24</sub> and vMC<sub>24</sub>NC are able to overcome the IFN-mediated resistance in H1HeLa cells, vMC<sub>24</sub>ΔL was not (Figure S1B). Replication of vMC<sub>24</sub>ΔL was markedly attenuated in H1HeLa cells compared to other Mengovirus constructs (Figure S2). To assess whether the vMC<sub>24</sub>ΔL induces early apoptosis in U87.luc cells, re-

stricting its replication, we stained infected cells for the Annexin V apoptosis marker. The Annexin V ratio was increased after 10 hpi in U87.luc cells infected with vMC<sub>24</sub>ΔL but was relatively lower than cells infected with vMC<sub>24</sub>. There was no statistically significant difference for annexin V staining between viruses with or without QVD, a pan-caspase inhibitor treatment that was used to suppress caspase-mediated apoptosis induction in both U87.luc (Figures S3A and S3B) and H1HeLa (Figures S3C and S3D) cells. These results suggested that vMC<sub>24</sub>ΔL did not induce an early apoptosis in U87.luc cells and that attenuated replication is cell type specific, mediated by a yet-unknown mechanism in U87.luc cells.

#### MicroRNA-detargeting attenuates Mengovirus cytotoxicity in murine glial cells *in vitro*

EMCV is serologically related to Mengovirus. EMCV replication in glial cells has been linked to the virus-mediated neurotoxicity.<sup>45</sup> We investigated Mengovirus replication in two mouse glial cell lines,

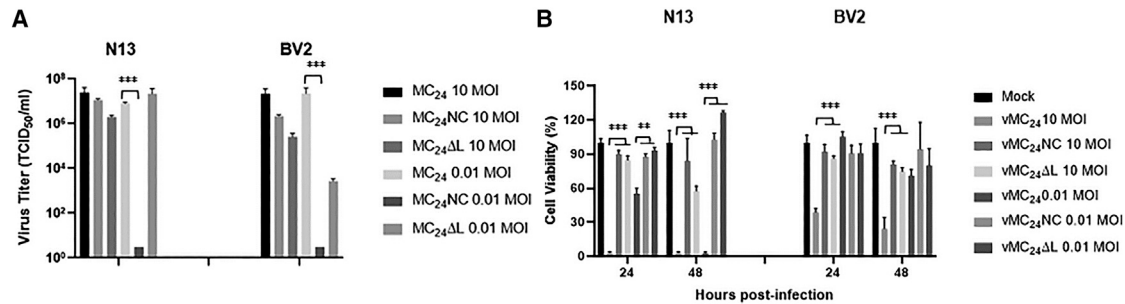


**Figure 2. MicroRNA detargeting thwarts Mengovirus replication in mouse microglia *in vitro***

(A) Total virus titers of vMC<sub>24</sub>NC and vMC<sub>24</sub>ΔL were evaluated (MOI 10, 0.01) in N13 cells and BV2 cells at 72 hpi. (B) Cytotoxicity of vMC<sub>24</sub>NC and vMC<sub>24</sub>ΔL was evaluated in N13 cells and BV2 cells at 10 and 0.01 MOI at 24 and 48 hpi. All experiments were repeated at least three times, and data are represented as mean values ± standard deviations. A p value of < 0.01 was considered significant (\*\*p < 0.01; \*\*\*p < 0.001).

N13 and BV2. Both cell lines were highly permissive to vMC<sub>24</sub> infection (Figure 2A), which significantly reduced cell viability (Figure 2B). vMC<sub>24</sub>ΔL replicated less efficiently in BV2 cells than in N13 cells after infection at 0.01 MOI, whereas vMC<sub>24</sub>NC failed to replicate in both mouse glial cells at low MOI, as evident by total virus titers at 72 hpi, suggesting that miRNA-detargeting restricts Mengovirus replication in mouse glial cells (Figure 2A). Although vMC<sub>24</sub>NC and vMC<sub>24</sub>ΔL were able to replicate in both mouse glial cell lines after infection at high MOI, both exhibited significantly reduced cytotoxicity compared to vMC<sub>24</sub> at 24 and 48 hpi (Figure 2B).

#### vMC<sub>24</sub>NC significantly reduces toxicity in a U87.luc xenograft model compared to vMC<sub>24</sub>ΔL

To compare the safety and therapeutic efficacy of vMC<sub>24</sub>NC and vMC<sub>24</sub>ΔL, athymic nude mice were implanted with human glioblastoma (U87.luc) cells *s.c.* Each mouse received a single *i.t.* injection of  $1 \times 10^8$  or  $1 \times 10^6$  median tissue culture infectious dose (TCID<sub>50</sub>) of either vMC<sub>24</sub>NC or vMC<sub>24</sub>ΔL. The control group received phosphate-buffered saline (PBS) alone (Figure 3). Tumors progressed rapidly in the control group and reached the criteria for euthanasia within 2 weeks post-treatment (Figure 3A, top). Tumor growth was suppressed in mice treated with  $1 \times 10^8$  TCID<sub>50</sub> vMC<sub>24</sub>ΔL; however 1 mouse developed hindlimb paralysis (HLP) on day 6, 2 mice were found dead on day 11, despite routine monitoring, and 1 mouse was euthanized because of large tumor volume on day 20 post-treatment (Figures 3B and 3C). Infectious virus was recovered from tumor, brain, spinal cord, and heart of the mouse that developed HLP at day 6 post-treatment, whereas no virus was recovered from the mice that were euthanized because of tumor burden or tumor ulceration (Figure 3D). Mice treated with  $1 \times 10^6$  TCID<sub>50</sub> of vMC<sub>24</sub>ΔL exhibited less efficiency in suppressing tumor growth than those treated with  $1 \times 10^8$  TCID<sub>50</sub> of vMC<sub>24</sub>ΔL, and 1 mouse was found dead on day 11 and the remaining 2 mice had to be euthanized on day 6 and day 22 post-treatment because of tumor ulceration. No infectious virus was recovered from tumor, brain, spinal cord, and heart tissues of the mice injected with vMC<sub>24</sub>ΔL that were euthanized because of tumor burden or tumor ulceration (Figure 3D). In contrast to vMC<sub>24</sub>ΔL, vMC<sub>24</sub>NC effectively regressed tumor volume at both

$1 \times 10^8$  and  $1 \times 10^6$  TCID<sub>50</sub> dosages. In the group that received  $1 \times 10^8$  TCID<sub>50</sub> of vMC<sub>24</sub>NC, tumors regressed in 3 out of 4 mice to the extent that they were no longer measurable. Tumor regrowth was observed in 1 mouse around day 40 post-treatment; however, complete tumor remission was observed in the other 2 mice for the duration of the study (Figure 3A). Tumor regression was observed in 1 out of 3 mice that received  $1 \times 10^6$  TCID<sub>50</sub> of vMC<sub>24</sub>NC, although tumor regrowth was noted on day 24 post-treatment and progressed thereafter, indicating a possible dose-dependent effect (Figure 3A). All other mice treated with vMC<sub>24</sub>NC ( $1 \times 10^8$  or  $1 \times 10^6$  TCID<sub>50</sub>) showed partial responses where tumor growth was delayed but tumors eventually grew to meet the criteria for euthanasia. Treatment with vMC<sub>24</sub>NC significantly improved overall survival compared to the control or vMC<sub>24</sub>ΔL-treated groups at both high and low dosages. There was an improvement in survival among mice injected with  $1 \times 10^8$  TCID<sub>50</sub> of vMC<sub>24</sub>NC compared to the  $1 \times 10^6$  TCID<sub>50</sub> group; however, the difference was not statistically significant ( $p = 0.0623$ ). (Figures 3B and 3C). To assess the replication of vMC<sub>24</sub>ΔL and vMC<sub>24</sub>NC in off-target tissues, 3 mice treated with a single *i.t.* injection of PBS or vMC<sub>24</sub>NC or vMC<sub>24</sub>ΔL at  $1 \times 10^8$  TCID<sub>50</sub> were euthanized on day 4 post-treatment and infectious virus titers were determined in tumor, brain, spinal cord, and heart (Figure 4). Replicable virus titer was recovered from all four tissues in the group injected with vMC<sub>24</sub>ΔL, indicating that deletion of the leader protein did not prevent viral replication in the tumors and the virus disseminated and replicated in brain, heart, and spinal cord. Viable titers of vMC<sub>24</sub>NC around  $1 \times 10^3$  TCID<sub>50</sub> were recovered from spinal cord tissue in 2 out of 3 mice; however, no infectious virus was recovered from brain and heart tissues in the group injected with vMC<sub>24</sub>NC, buttressing the evidence that miRNA-detargeting improves the safety of vMC<sub>24</sub> in tumor-bearing immunocompromised mice.

#### MicroRNA-detargeting is a superior strategy for improving the safety profile of oncolytic Mengovirus

Athymic nude mice received a single *i.c.* injection of vMC<sub>24</sub>NC or vMC<sub>24</sub>ΔL to assess their toxicity profiles against each other. Mice were injected with a single dose of  $1 \times 10^7$ ,  $1 \times 10^5$ , or  $1 \times 10^3$

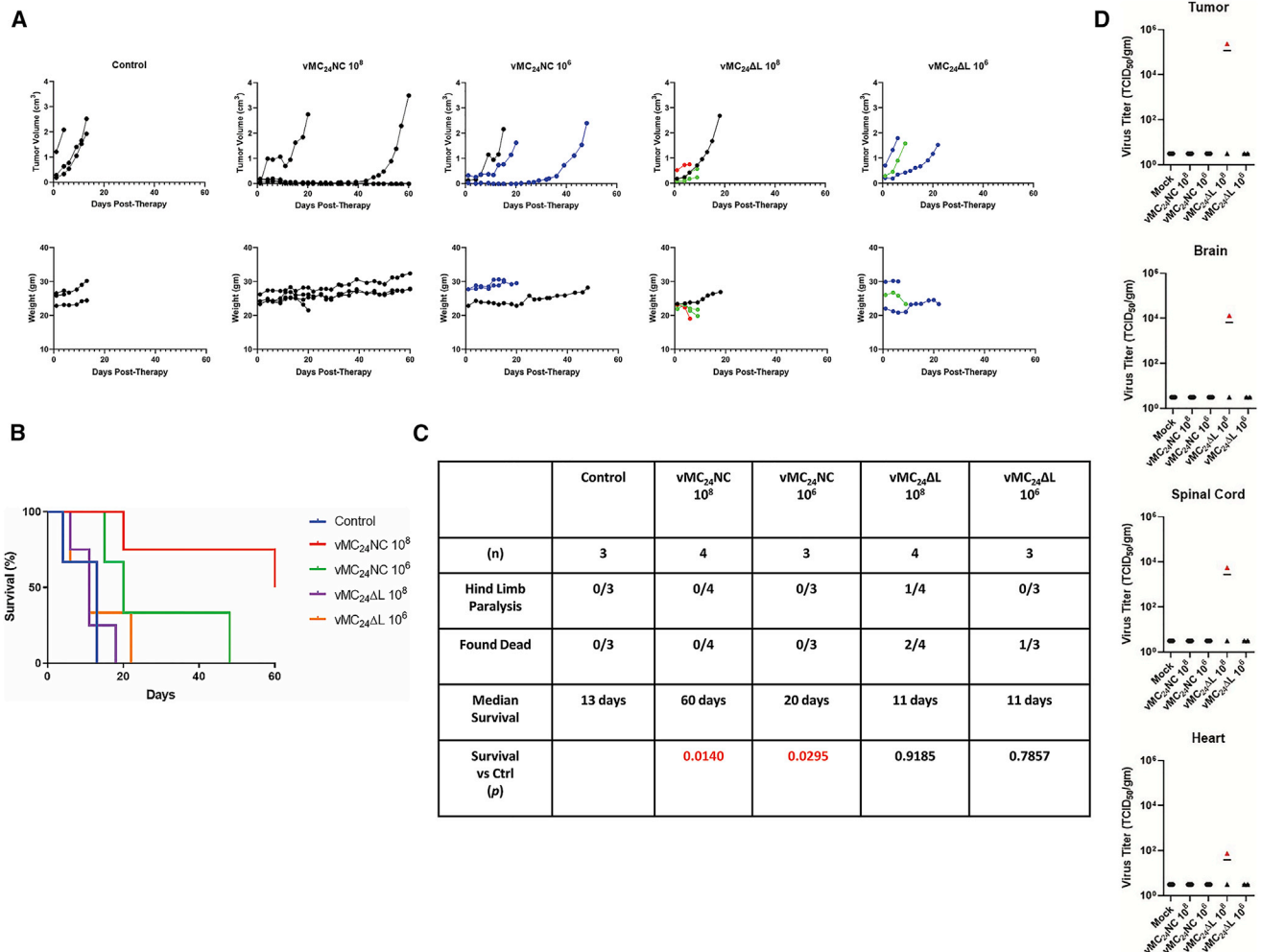


**Figure 3. vMC<sub>24</sub>ΔL is toxic in U87.luc xenograft model**

Athymic nude mice bearing s.c. U87.luc tumors were treated with a single i.t. injection of  $1 \times 10^6$  or  $1 \times 10^8$  TCID<sub>50</sub> vMC<sub>24</sub>NC or vMC<sub>24</sub>ΔL. (A, top) Disease burden was monitored by calculating tumor volume versus time using repeat caliper measurements. (A, bottom) Weight was monitored for the duration of the experiment. (B) Overall survival of control (n = 3)-, vMC<sub>24</sub>NC  $1 \times 10^8$  (n = 4)-, vMC<sub>24</sub>NC  $1 \times 10^6$  (n = 3)-, vMC<sub>24</sub>ΔL  $1 \times 10^8$  (n = 4)-, and vMC<sub>24</sub>ΔL  $1 \times 10^6$  (n = 3)-treated mice were assessed with Kaplan-Meier survival curves. (C) Tabulation of cause of death/euthanasia aside from tumor volume in all treated mice, median survival, and significance of overall survival benefit in control versus vMC<sub>24</sub>NC- or vMC<sub>24</sub>ΔL-treated mice based on log rank analyses. (D) Infectious virus titers within the tumor, brain, spinal cord, and heart were determined at the time of euthanasia. Virus titers are represented as mean values  $\pm$  standard deviations. Data points in red, blue, and green represent animals that developed HLP, tumor ulceration, and sudden death, respectively.

TCID<sub>50</sub>, of vMC<sub>24</sub>NC or vMC<sub>24</sub>ΔL. Control group mice received a single i.c. injection of an equivalent volume of PBS. All mice in the control group survived until the end of the experiment and showed no signs of neurological complications, indicating that the i.c. injection alone did not lead to any neurological impairment or other forms of toxicity. Mice injected with vMC<sub>24</sub>ΔL rapidly developed clinical signs of toxicity and either were found dead or developed HLP. The overall survival rate in mice injected with vMC<sub>24</sub>ΔL at all three dosages was significantly lower compared to the control group or groups that received equivalent dosages of vMC<sub>24</sub>NC (Figures 5A and 5B). All mice in the group injected with  $1 \times 10^7$  TCID<sub>50</sub> of vMC<sub>24</sub>ΔL died within the first week post-treatment, among which 2 mice

were found dead on day 5, and 2 developed HLP on day 7 post-treatment. In the group that was injected with  $1 \times 10^5$  TCID<sub>50</sub> of vMC<sub>24</sub>ΔL, 3 mice were found dead on day 5 and 1 mouse was in a moribund state on day 9 post-treatment. Even the low dose of  $1 \times 10^3$  TCID<sub>50</sub> of vMC<sub>24</sub>ΔL resulted in toxicity, although it was slightly delayed compared to the high-dose groups. In this group, 2 mice developed HLP on day 7 and 1 on day 22 post-treatment, and 1 animal was found dead on day 11 post-treatment. The level of viremia on day 2 post-virotherapy was lower in mice injected with vMC<sub>24</sub>ΔL compared to mice injected with vMC<sub>24</sub>NC (Figure 5C), likely because of attenuated replication of vMC<sub>24</sub>ΔL. Infectious virus was recovered from the brain, spinal cord, and heart of all animals injected with

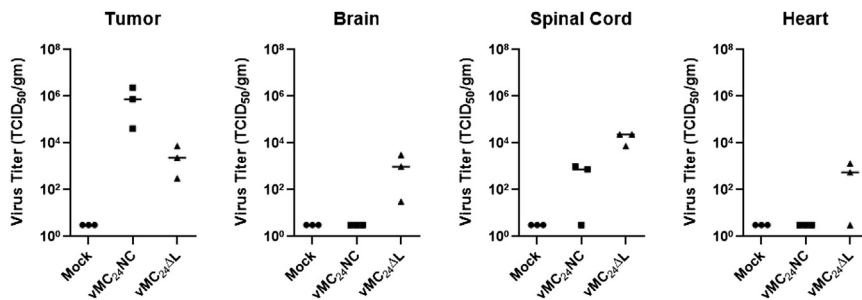


**Figure 4. vMC<sub>24</sub>ΔL replicates more efficiently in neural and cardiac tissue than vMC<sub>24</sub>NC**

Athymic nude mice bearing s.c. U87.luc tumors were treated with a single i.t. injection of PBS (n = 3) or  $1 \times 10^8$  TCID<sub>50</sub> vMC<sub>24</sub>NC (n = 3) or vMC<sub>24</sub>ΔL (n = 3). Mice were euthanized 4 days post-injection, and the infectious virus titers within the tumor, brain, spinal cord, and heart were determined. Virus titers are represented as mean values  $\pm$  standard deviations.

vMC<sub>24</sub>ΔL irrespective of the dose of virus they received, with the exception of a few mice injected with  $1 \times 10^3$  TCID<sub>50</sub> where no virus was recovered from heart tissue (Figure 5D). In the groups that were injected with  $1 \times 10^7$  and  $1 \times 10^5$  TCID<sub>50</sub> of vMC<sub>24</sub>NC, 1 mouse each had to be euthanized because of their moribund condition on day 9 and day 55 post-treatment, respectively. Virus could be isolated from the brain and spinal cord of the mouse euthanized on day 9 and from the spinal cord only of the mouse that was euthanized on day 55 post-treatment. Equivalent virus titers of both vMC<sub>24</sub>NC and vMC<sub>24</sub>ΔL were obtained from liver tissue, indicating that it did not act as a site to boost replication of either virus, leading to toxicity. No virus was recovered from skeletal muscle for either of the virus groups. No toxicity was observed in the group that was injected with the low dose of vMC<sub>24</sub>NC ( $1 \times 10^3$  TCID<sub>50</sub>), and all animals survived until the end of the study. To examine the cause of toxicity in the 2 mice that were injected with vMC<sub>24</sub>NC and had to be euthanized because of development of a moribund condition, viral RNA was isolated from the brain, spinal cord, and heart and NCRs carrying miRNA target (miRT) sequences amplified by nested PCR. All 6 miRT sequences, including 2 miRT sequences in the 5' NCR (Figure 6A) and 4 miRT sequences in the 3' NCR (Figure 6B), were completely deleted in the virus isolated from all three tissues of the mouse injected with  $1 \times 10^7$  TCID<sub>50</sub> of vMC<sub>24</sub>NC. Similarly, all 6 sequences were completely deleted from 5' and 3' NCRs in the viruses isolated from spinal cord and heart of the mouse injected with  $1 \times 10^5$  TCID<sub>50</sub> of vMC<sub>24</sub>NC. The muscle/cardiac-specific miRT-133 (2 copies) and miRT-208 (2 copies) sequences in the 3' NCR remained intact in the virus recovered from the brain of the mouse injected with  $1 \times 10^5$  TCID<sub>50</sub> of vMC<sub>24</sub>NC; however, both miRT-124 sequences were completely deleted from its 5' NCR (Figure 6).

## DISCUSSION

A variety of oncolytic viruses have progressed into clinical trial investigations, while many others remain under investigation in the pre-clinical phase to treat various cancer types.<sup>46–49</sup> A wide range of strategies are being used to enhance both safety and efficacy of oncolytic viruses in different classes of viruses. The broad range of tissue and host tropism of Mengovirus makes this virus feasible to test for its oncolytic efficacy in different syngeneic murine tumor models as well as human tumors in xenograft models.<sup>12</sup> Mengovirus has a rapid lytic cycle, allowing it to reach high titers in tumors after both i.t. and systemic delivery.<sup>12</sup> A low level of sero-prevalence in humans against Mengovirus

acts in favor of the virus, because it is a crucial factor in avoiding loss of therapeutic efficacy due to rapid antibody-mediated neutralization of the virus by pre-existing antiviral immunity, when delivered systemically.<sup>28</sup> Mengoviruses with a truncated (vMC<sub>24</sub>) and a deleted (vMC<sub>0</sub>) poly(C) tract in the 5' NCR have been shown to induce protective immunity against EMCV-like viruses with no adverse effects.<sup>28–31</sup> Although studies demonstrated that vMC<sub>24</sub> is safe to be used in animals for vaccination, our lab has shown that vMC<sub>24</sub> is still capable of resulting in significant virus-mediated toxicity when used in an immunocompetent mouse plasmacytoma MPC-11 tumor model, entailing further efforts to eliminate viral toxicity.<sup>12</sup> The toxicity of vMC<sub>24</sub> in the MPC-11 mouse model is likely due to high viremia following replication within the tumor bed seeding off-target tissues. Picornavirus toxicity can be subdued through miRNA-mediated detargeting to prevent viral replication in off-target tissues, which is a well-studied technique.<sup>1,13,50–52</sup> This technique has worked very effectively for improving the safety profile of Mengovirus. The dual-detargeted Mengovirus, vMC<sub>24</sub>NC, showed potent therapeutic efficacy in a syngeneic plasmacytoma MPC-11 model without significant neuro- and cardiotoxicity.<sup>12</sup> However, the low fidelity of the viral RNA polymerase can lead to mutations throughout the genome, and the selective pressure exerted by using a host-mediated targeting mechanism on viral fitness makes the stability of the miRNA targets inserted into the NCRs of Mengovirus a potential safety concern in immunocompromised hosts. Mutations within miRNA target sequences can unhinge the safety lock against viral toxicity, although optimized localization of the targets within the virus genome, using completely complementary target sequences, as well as redundancy in target use can minimize the potential for escape mutant development.<sup>12</sup> Achieving good efficacy as an oncolytic agent requires injection of high doses of Mengovirus versus that required for immunization, necessitating alternative strategies to reduce viral toxicity in animals.

Attenuation of virus through deletion of viral genes that are non-essential for viral replication is a commonly used strategy for developing safe oncolytic viruses.<sup>53</sup> Unlike large DNA viruses like vaccinia and herpes simplex virus that have several virulence genes that can be manipulated to attenuate the virus, picornaviruses have a small RNA genome, limiting the viral genes that can be manipulated for attenuation. Mengovirus proteins L (encoded by *leader* gene) and 2A (encoded by *2A* gene) are considered viral safety proteins that allow viral replication by preventing immediate-early activation of IFN

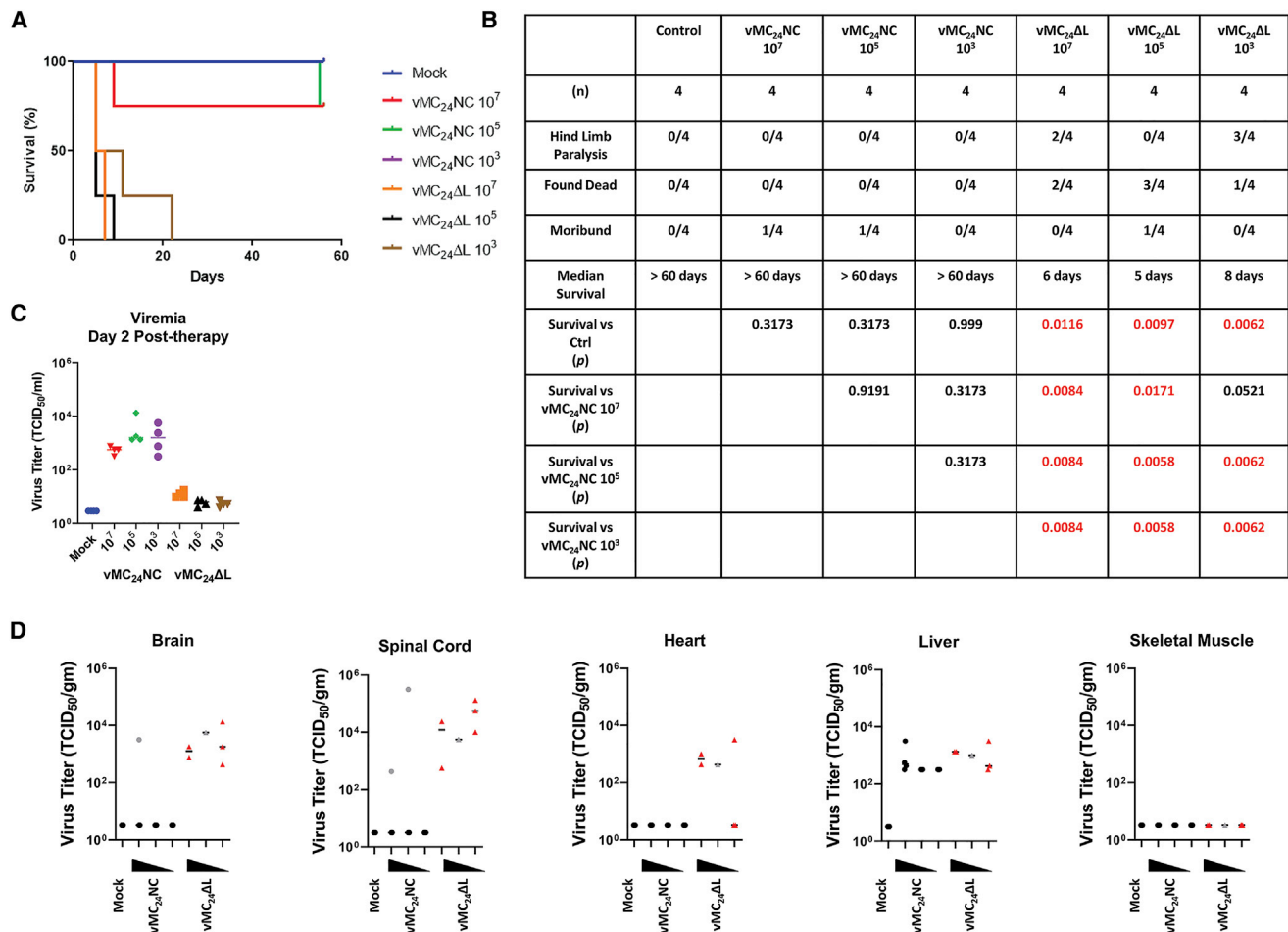


**Figure 5. Intracranial delivery of vMC<sub>24</sub>ΔL is lethal in athymic nude mouse**

Athymic nude mice were treated with a single i.c. injection of  $1 \times 10^7$ ,  $1 \times 10^5$ , or  $1 \times 10^3$  TCID<sub>50</sub> of vMC<sub>24</sub>NC or vMC<sub>24</sub>ΔL (n = 4 in each group). (A) Overall survival of control and vMC<sub>24</sub>NC- and vMC<sub>24</sub>ΔL-treated mice was assessed with Kaplan-Meier survival curves. (B) Tabulation of causes of death/euthanasia in all mice, median survival rates, and significance of overall survival benefit based on log rank analyses. (C) Plasma viral loads in virus-treated mice were determined on day 2 after therapy. (D) Viral loads in tissues harvested at the time of euthanasia were determined. Data points in red and gray represent animals that were euthanized because of the development of HLP and moribund condition, respectively. Virus titers in both sera and tissue samples are represented as mean values ± standard deviations.

response that can push the host cells into the antiviral state and inhibiting caspase-mediated apoptosis in infected cells.<sup>33,34,54</sup> Considering the role of the L and 2A proteins in determining Mengovirus virulence, we deleted these genes to generate vMC<sub>24</sub>ΔL and vMC<sub>24</sub>Δ2A, respectively. Deletion of the 2A gene severely impacted replicability of Mengovirus in BHK-21 cells, as the maximum virus titer at 72 hpi was ~3 log fold lower than vMC<sub>24</sub> (Y.R.S., unpublished data). As the ability of the virus to replicate to high titers in tumor cells is a critical component to achieve direct viral oncolysis leading to good efficacy, we discontinued our analyses of vMC<sub>24</sub>Δ2A for oncolytic virotherapy; however, its potential as a cancer vaccine remains to be investigated. Contrary to vMC<sub>24</sub>Δ2A, vMC<sub>24</sub>ΔL was able to infect and replicate in BHK-21 and U87.luc cells. vMC<sub>24</sub>ΔL has been shown to be non-toxic when injected into immunocompetent mice.<sup>34</sup> Unlike vMC<sub>24</sub>NC the safety of vMC<sub>24</sub>ΔL is based on the permanent deletion of the *leader* gene, limiting the possibility of gener-

ation of escape variants. The vMC<sub>24</sub>ΔL loses its ability to antagonize type I IFN responses in infected host cells because of the absence of the leader protein,<sup>34</sup> which can likely improve its safety, since the virus will be attenuated in normal cells with intact IFN response pathways but can exploit the defective IFN response pathways in a variety of cancer cells.<sup>55,56</sup> EMCV replication in glial cells is known to produce toxic oxidative radicals that have been linked with virus-mediated neurotoxicity.<sup>45</sup> As Mengovirus is a strain of EMCV and serologically identical to EMCV, we hypothesize that a similar mechanism is involved in vMC<sub>24</sub> neurotoxicity. Deletion of the *leader* gene from Mengovirus to enhance its safety appeared to be an empirical strategy based on the known functions of the leader protein and its proven safety in immunocompetent mice. This prompted us to explore whether the deletion of the *leader* gene would attenuate the Mengovirus enough to be safe in immunodeficient mouse models yet retain its therapeutic efficacy as an oncolytic virus.

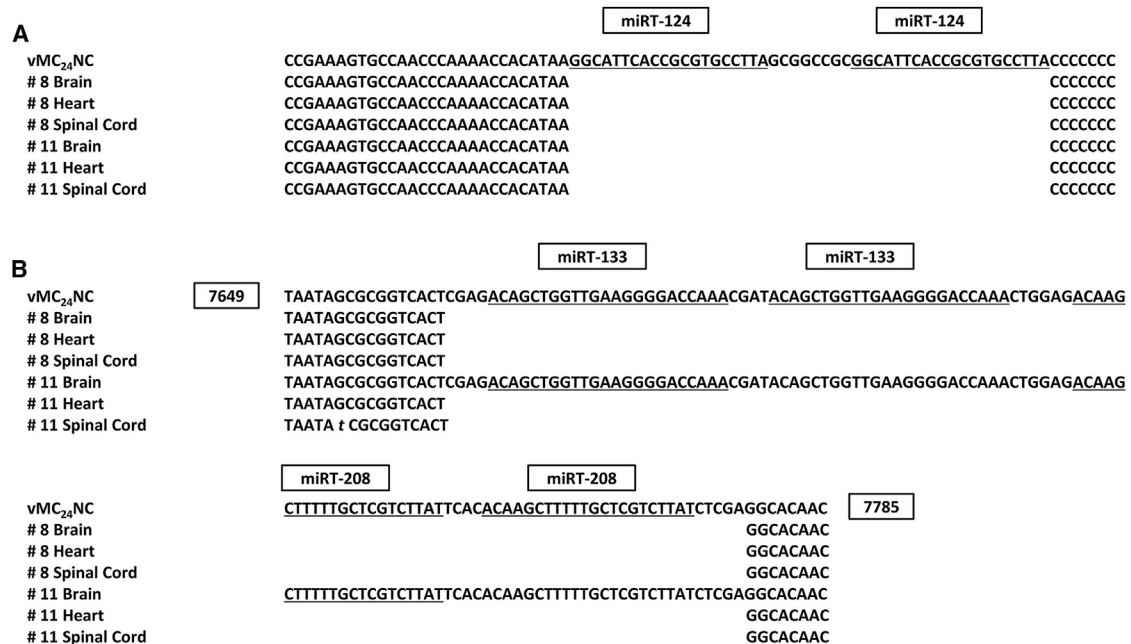


**Figure 6. Genetic stability of miRNA target sequences after intracranial delivery**

Viral RNA was isolated from the clarified lysates of brain, heart, and spinal cord tissues isolated at terminal end points. Mice #8 and #11 received a single i.c. dose of  $1 \times 10^7$  and  $1 \times 10^5$  TCID<sub>50</sub>, respectively. Regions containing the miRTs were amplified via RT-PCR. PCR samples were directly sequenced to determine the consensus sequence. (A) Consensus sequences with mutations obtained from 5' PCR amplicons. (B) Consensus sequences with mutations obtained from 3' PCR amplicons. The miRT sequences are indicated by underlined text, and substitution mutation is shown in boldface and lowercase text. Sequences are aligned to indicate completely deleted bases from the viral genomes.

In this study we compared miRNA-detargeting against deletion of the *leader* virulence gene in Mengovirus as safety strategies in engineering oncolytic Mengovirus. We tested vMC<sub>24</sub>ΔL replication in mouse glial cells, where the virus replication was suboptimal in BV2 mouse glial cells compared to vMC<sub>24</sub> but not in N13 mouse glial cells, while vMC<sub>24</sub>NC failed to replicate in both mouse glial cells, at 0.01 MOI *in vitro* (Figure 2C). Brain tissue including microglia has been reported to express high levels of miRNA-124.<sup>57</sup> The BV2 cells are known to express miRNA-124, which explains the failure of vMC<sub>24</sub>NC to replicate in these cells;<sup>58</sup> however, its expression level in N13 cells has not been reported. The BV2 and N13 cell lines are also derived from different strains of mice, which could attribute to the innate differential activity level of cellular pathways, including type I IFN response and apoptotic pathways affecting their permissiveness to vMC<sub>24</sub>ΔL.<sup>59,60</sup> Immortalized microglia like BV2 have been shown to be transcriptionally less responsive than primary microglia, which hints at the possibility of a differential response by glial cells in GBM patients.<sup>61,62</sup> We further tested the toxicity of vMC<sub>24</sub>NC and vMC<sub>24</sub>ΔL *in vivo*. Intratumoral injection of vMC<sub>24</sub>NC in U87.luc xenograft-bearing athymic nude mice resulted in complete and partial tumor responses and a significant increase in overall survival (Figure 3), whereas i.c. injection of vMC<sub>24</sub>NC resulted in minimal toxicity (Figure 5). Contrary to that, vMC<sub>24</sub>ΔL suppressed the U87.luc tumor growth but resulted in viral toxicity reducing the overall survival rate significantly, when injected both directly into s.c. U87.luc xenografts

(Figure 3) and i.c. (Figure 5). Although at 2 days post i.c. administration the level of viremia among animals injected with vMC<sub>24</sub>NC was higher relative to those injected with vMC<sub>24</sub>ΔL (Figure 5C), the toxicity observed and recovery of infectious virus from tissues in vMC<sub>24</sub>ΔL-injected mice suggest that peak viremia likely occurred later. Together these results indicate that miRNA-detargeting is a superior strategy over deletion of the virulence genes like the *leader* gene for enhancing safety of oncolytic Mengovirus. Also of note is that toxicity in mice treated with vMC<sub>24</sub>NC was only observed following i.c. injection, solidifying the precedent for continued development of vMC<sub>24</sub>NC for clinical translation against certain indications. Nevertheless, miRNA targets in vMC<sub>24</sub>NC are still prone to mutation that can lead to toxicity (Figure 6), and therefore continued development of safer versions of Mengovirus or combination with immunostimulatory therapies is likely required for translation against brain cancers, although treatment of resected tumor cavities may be a viable option. Even though the mutation rate is high in RNA viruses,<sup>63</sup> oncolytic RNA viruses should theoretically still be able to execute the therapeutic effect and be cleared by the immune system before generation of toxic revertant strains. Unlike our earlier study,<sup>12</sup> we observed Mengovirus toxicity due to loss of miRNA targets at an earlier stage in our current i.c. *in vivo* study. Our results showed that the miRNA targets in the 3' NCR of Mengovirus genome were cleaved off at the restriction sites on either ends of these target sequences, which led to toxicity in some of these mice (Figure 6B).

These restriction sites might be acting as scar sequences, which may result in enhanced deletion of miRNA targets in vMC<sub>24</sub>NC. It will be interesting to see if seamless cloning of these miRNA targets into the NCRs of the viral genome can improve the stability of these inserts. Alternatively, the length of poly(C) can be curtailed to maintain the Mengovirus genome length at its original size to improve the stability of miRNA targets, provided that the construct's replicability in cancer cells remains unaltered. Oncolytic Coxsackievirus A21 has been successfully detargeted to attenuate its cardiotropic virulence, while maintaining genome length, by replacing the spacer region downstream of the internal ribosome entry site with tissue-specific miRNAs. The miRNA response element was stable even after multiple cell passages and did not alter the virus replication, which indicates that the integrity of miRNA targets can be preserved.<sup>14</sup> Finally, the correlation between status of the immune landscape and rate of mutations in Mengovirus genome remains to be explored.

The vMC<sub>24</sub>ΔL which has been shown to be safe in immunocompetent mice,<sup>34</sup> is toxic in athymic nude mice with deficient adaptive immunity, emphasizing the critical role of immune status in determining viral toxicity. This is consistent with some other viruses like oncolytic Reovirus, which has been shown to be lethal in the newborn<sup>64</sup> and immunocompromised animals<sup>65</sup> but safe in adult immunocompetent animal models.<sup>64</sup> It will be interesting to see if vMC<sub>24</sub>ΔL can be detargeted by inserting miRNA targets in the NCRs, which could also benefit the stability of miRNA targets due to the curtailed genome size in vMC<sub>24</sub>ΔL, provided that the virus retains its efficacy as an oncolytic agent. Going further, therapeutic efficacy of vMC<sub>24</sub>ΔL in syngeneic immunocompetent models remains to be explored, as the virus has been shown to be safe in immunocompetent mice.<sup>34</sup>

The GBM is a difficult tumor type to treat because of several factors such as tumor heterogeneity, blood-brain barrier, and immunosuppressive TME and is in dire need of new effective therapeutics. Mengovirus has a natural tropism for neuronal tissue, but its replication in healthy neuronal cells can be prevented via the miRNA-detargeting strategy to eliminate viral toxicity. In the human GBM U87 xenograft model, vMC<sub>24</sub>NC showed good therapeutic efficacy and safety. Furthermore, vMC<sub>24</sub>NC can be tested in an orthotopic syngeneic mouse GBM model in combination with immunotherapies, lower the dose of virus required, to maximize the therapeutic efficacy and safety. With a proven record as a vaccine candidate<sup>29-31</sup> and ability to cross the blood-brain barrier as evident in our study in the U87.luc subcutaneous xenograft model where the virus was isolated from brain and spinal cord even when injected into tumors, Mengovirus warrants further development as a therapeutic for GBM. Although the local immunosuppressive environment in and around GBM tumor is expected to provide a privileged site for oncolytic virus replication, most clinical studies are documented in immunocompromised patients, which makes it more critical to strike a balance between safety and efficacy when engineering oncolytic viruses.

In conclusion, miRNA-detargeting is still the best available strategy to improve the safety of oncolytic Mengovirus, because both vMC<sub>24</sub>

and vMC<sub>24</sub>ΔL led to toxicity when used in tumor models. Although vMC<sub>24</sub> has been shown to be safe in animals in the absence of tumors<sup>31</sup> and vMC<sub>24</sub>ΔL has been shown to be safe in immunocompetent mice,<sup>34</sup> vMC<sub>24</sub>NC remains an appealing and viable oncolytic virus candidate that strikes a better balance between safety and efficacy. Although we observed neurotoxicity in a couple of mice following direct i.c. injection of vMC<sub>24</sub>NC due to deletion of miRNA target sequences, the virus proved effective and safe in both mouse and human peripheral tumor models (U87 and MPC-11).<sup>12</sup> In addition to factors like tumor size, the initial viral distribution within a tumor, and the subsequent levels of viremia that we previously speculated to play a critical role in determining Mengovirus toxicity, immune status of animals also appears to matter. Additional studies will be needed to elucidate the complex interaction between Mengovirus and the host immune system that impact viral toxicity. Differential toxicities of vMC<sub>24</sub>ΔL in immunocompetent and immunodeficient mice raise a red flag and underscore the importance of considering immune status in cancer patients when moving these viruses into clinic.

## MATERIALS AND METHODS

### Cells

BHK-21 (ATCC CCL-10), H1HeLa (ATCC CRL-1958), and U87-MG (ATCC HTB-14) cell lines were purchased from the American Type Culture Collection (ATCC; Manassas, VA, USA). BHK-21 and U87-MG cells were grown in Dulbecco's modified Eagle's medium (DMEM; SH30022.01, Thermo Scientific, Waltham, MA, USA) supplemented with 10% fetal bovine serum (FBS). We performed no further authentication of the cell lines, since ATCC routinely tests morphology, karyotype, and species. All cells routinely tested negative for mycoplasma contamination. U87.luc are U87-MG cells expressing luciferase and were generated in our lab following a protocol that has been described previously.<sup>66</sup> BV2<sup>59</sup> and N13<sup>60</sup> cells were a kind gift from Dr. Evanthis Galanis' laboratory (Mayo Clinic, Rochester, Department of Molecular Medicine) and have been reported earlier.<sup>67,68</sup> Both BV2 and N13 cells were cultured in RPMI 1640 medium (10-040-CV, Thermo Scientific, Waltham, MA, USA) with 10% FBS. All cell lines were also supplemented with 100 U/mL penicillin and 100 µg/mL streptomycin added to the respective media.

### pMC<sub>24</sub>ΔL plasmid

The pF/R-wt and RZ-pMwt plasmids were kind gifts from Ann C. Palmenberg (University of Wisconsin, Department of Biochemistry and the Institute for Molecular Virology), and their construction has been described before.<sup>69,70</sup> Generation of the pMC<sub>24</sub> with a truncated homopolymeric poly(C) tract in the 5' NCR of Mengovirus genome has been described previously.<sup>12</sup> The plasmid pMC<sub>24</sub>NC was generated by cloning two copies of miRNA target sequences complementary to miR-124 (enriched in nervous tissue) in the 5' NCR and two copies of sequences complementary to miR-133 and miR-208 (enriched in cardiac/skeletal muscle tissue) in the 3' NCR of Mengovirus genome as described previously.<sup>12</sup> The plasmid pMC<sub>24</sub>ΔL was generated by splice overlap extension PCR where the

internal primers were designed so that the overlapping ends span the junction of coding sequences with exclusion of the target nucleotide sequence encoding amino acids 12–52 in the leader protein, which included the zinc finger binding domain and phosphorylation site that have been shown to be critical for functioning of the Mengovirus leader protein.

#### Generation of vMC<sub>24</sub>ΔL virus

A total of  $4 \times 10^5$  BHK-21 cells were seeded per well into 6-well plates and incubated at 37°C in 5% CO<sub>2</sub> overnight. BHK-21 cells were transfected on the next day with a total of 2.5 μg of pMC<sub>24</sub>ΔL per well, using Mirus TransIT-2020 transfection reagent (MIR 5400, Mirus Bio, Madison, WI, USA) according to the manufacturer's instructions. Cells were scraped into the supernatant when cytopathic effects (CPEs) were apparent (24–72 h post-transfection). Samples were subjected to three freeze-thaw cycles, the cellular debris was removed by low-speed centrifugation, and the cleared lysate was filtered through a 0.22-μm filter and passaged onto BHK-21 cells. Filtered viral supernatant was layered onto a 30% sucrose cushion and concentrated through ultracentrifugation at 27,000 rpm for 1 h at 4°C. The viral pellet was resuspended in PBS. Virus stocks of vMC<sub>24</sub> and vMC<sub>24</sub>NC were generated following a similar protocol, except the viruses were rescued and grown in H1Hela cells instead of BHK-21 cells. Viral RNA was isolated from all virus stocks with a QiaAmp Viral RNA Mini Kit (52904, QIAGEN, Valencia, CA, USA) according to the manufacturer's instructions. Deletion of *leader* gene in vMC<sub>24</sub>ΔL and regions containing the miRNA inserts in vMC<sub>24</sub>NC were amplified with the Titan one-tube reverse transcriptase-PCR (RT-PCR) system (11855476001; Roche Applied Science, Indianapolis, IN, USA), and the integrity of the edited sequence was verified via sequencing.

#### Virus titration

A total of  $1 \times 10^4$  BHK-21 cells were seeded per well into 96-well plates and grown at 37°C in 5% CO<sub>2</sub>. At 24 hpi, 10-fold serial dilutions of each virus stock were made and 100 μL of each dilution was added to each of eight replicate wells. The cells were incubated at 37°C in 5% CO<sub>2</sub> for 72 hpi. The cells were visually assessed for CPE and scored as positive or negative. The TCID<sub>50</sub> per milliliter was calculated with the Spearman and Kärber equation. Stocks of all viruses were titrated on BHK-21 cells to determine TCID<sub>50</sub> per milliliter.

#### Cell viability assay

The 3-(4,5-dimethylthiazolyl-2)-2,5-diphenyltetrazolium bromide (MTT) (30-1010K, ATCC, Manassas, VA, USA) analysis was used to measure vMC<sub>24</sub>, vMC<sub>24</sub>NC, or vMC<sub>24</sub>ΔL cytotoxicity in all cell lines against mock-infected control. Cells were infected for 2 h at 37°C in 5% CO<sub>2</sub>, followed by replacement with fresh complete growth medium. Cell viability was analyzed at some or all time points starting from 2, 4, 6, 8, 10, 24, 48 until 72 hpi in BHK-21 and U87.luc cells. Cell viability of BV2 and N13 cells was analyzed in a similar manner at 24 and 48 hpi.

#### Viral replication curves

BHK-21, U87.luc, N13, and BV2 cells were infected at an MOI of 10 or 0.01 for 2 h at 37°C in 5% CO<sub>2</sub>, followed by removal of the inoculum and addition of fresh complete growth medium. At 2, 4, 6, 8, 10, 24, 48, and 72 hpi, cells were scraped into the supernatant and samples were frozen at –80°C. Once all samples had been collected, they underwent three quick freeze-thaw cycles in liquid nitrogen and the cellular debris was removed through low-speed centrifugation. Cleared lysates were titrated on BHK-21 cells as described above. A similar protocol was followed when investigating virus titers in BV2 and N13 cells at 72 hpi.

#### Animal experiments

The Mayo Clinic Institutional Animal Care and Use Committee approved and monitored all animal studies. All *in vivo* studies used 6-week-old female athymic nude mice that were purchased from Envigo (Indianapolis, IN, USA). For i.t. administration studies,  $5 \times 10^6$  washed U87.luc cells were implanted subcutaneously (s.c.) into athymic nude mice. When tumors reached an average diameter of 0.5 cm, mice were treated with PBS or  $1 \times 10^8$  or  $1 \times 10^6$  TCID<sub>50</sub> of vMC<sub>24</sub>NC or vMC<sub>24</sub>ΔL diluted in PBS. At 4 days post-treatment, 3 mice per group (including controls) were euthanized, and all other animals were analyzed for survival. Tissues were harvested and immediately flash frozen for virus titration. All tumor-bearing mice were observed and weighed, and tumor size was measured 3 times a week with a handheld caliper. Blood was obtained through cardiac puncture at the time of euthanasia. Harvested tissues were immediately sectioned into a vessel containing 10% neutral buffer formalin and placed at room temperature. For i.c. administration studies, mice were treated with PBS or  $1 \times 10^7$ ,  $1 \times 10^5$ , or  $1 \times 10^3$  TCID<sub>50</sub> of vMC<sub>24</sub>NC or vMC<sub>24</sub>ΔL diluted in PBS. All treated mice were observed and weighed until they met one of the criteria for euthanasia, such as HLP or the inability to eat or drink because of moribund condition or the end point of the experiment. Mice were euthanized and tissues were harvested as described above.

#### Plasma virus titration

Terminal blood samples were collected via intracardiac puncture, whereas intermediate blood samples were collected from the submandibular vein. Blood was collected in a BD Microtainer tube with a lithium heparin and plasma separator (365958, BD Biosciences). Plasma was collected after centrifugation according to the manufacturer's instructions. Viral loads were determined by titrating virus on BHK-21 cells as described above, and the TCID<sub>50</sub> per milliliter was calculated.

#### Tissue virus titration and miRNA target genetic stability analysis

For i.t. administration studies, to quantify virus in tissues at 4 days post-treatment, whole organs from mice were harvested and stored at –80°C until further processing. Organs were weighed and homogenized with Kimble Chase Kontes pellet pestles (K749520, Fisher Scientific) and suspended in a total volume of 1 mL of DMEM. Tissue suspensions were subjected to three freeze-thaw cycles and centrifuged. The cleared tissue lysates were titrated on BHK-21 cells as

described above, and the TCID<sub>50</sub> per gram of tissue was calculated. For all other animals in i.t. and i.c. administration studies, half of the organs were sectioned at terminal end point and stored at  $-80^{\circ}\text{C}$  until further processing as described above to prepare tissue suspension for virus titration. Viral RNA was isolated from cleared tissue lysates with a QiaAmp Viral RNA Mini Kit (QIAGEN, Valencia, CA, USA) according to the manufacturer's instructions. cDNA was synthesized with SuperScript III First-Strand Synthesis SuperMix (18080-400, Life Technologies, Grand Island, NY, USA) according to the manufacturer's instructions. Regions containing the miRNA target insert sequences were amplified with an Expand High-Fidelity PCR kit (04738250001, Roche Applied Science, Indianapolis, IN, USA) according to the manufacturer's instructions.

### Statistical analysis

GraphPad Prism software, version 5.0a (GraphPad Software, La Jolla, CA, USA), was used for data analysis and graphical representations. Two-tailed unpaired Student *t* tests assuming unequal variances were used for statistical analysis of virus titers and cell viability assay, and  $p < 0.05$  was considered statistically significant. Survival curves were plotted according to the Kaplan-Meier method, and the survival rates across treatment groups were compared with log rank tests.

### Data availability

Data are available from the corresponding author upon reasonable request.

### SUPPLEMENTAL INFORMATION

Supplemental information can be found online at <https://doi.org/10.1016/j.omto.2021.08.011>.

### ACKNOWLEDGMENTS

We thank Ann C. Palmenberg of the University of Wisconsin, Department of Biochemistry and Institute for Molecular Virology, for the kind gifts of the pF/R-wt and Rz-pMwt plasmids and communications regarding their use. We also thank Dr. Evanthia Galanis, Department of Molecular Medicine, Mayo Clinic, Rochester, for BV2 and N13 cells. We thank Eugene Bah, Department of Molecular Medicine, Mayo Clinic, Rochester, for generating U87.luc cells. This publication was made possible by grant number CA207386 from NCI, United States and Mayo Clinic funding, and its contents are solely the responsibility of the authors and do not necessarily represent the official views of the NIH or Mayo Clinic.

### AUTHOR CONTRIBUTIONS

Y.R.S., S.J.R., and A.J.S. conceived the project. Y.R.S. performed *in vitro* experiments. R.A.N. and Y.R.S. performed *in vivo* experiments. Y.R.S., S.J.R., and A.J.S. wrote the manuscript. S.J.R. and A.J.S. supervised the project.

### DECLARATION OF INTERESTS

The authors declare no competing interests.

### REFERENCES

- Ruiz, A.J., and Russell, S.J. (2015). MicroRNAs and oncolytic viruses. *Curr. Opin. Virol.* *13*, 40–48.
- Bell, J.C., and Kirn, D. (2008). MicroRNAs fine-tune oncolytic viruses. *Nat. Biotechnol.* *26*, 1346–1348.
- Lee, C.Y., Rennie, P.S., and Jia, W.W. (2009). MicroRNA regulation of oncolytic herpes simplex virus-1 for selective killing of prostate cancer cells. *Clin. Cancer Res.* *15*, 5126–5135.
- Hikichi, M., Kidokoro, M., Haraguchi, T., Iba, H., Shida, H., Tahara, H., and Nakamura, T. (2011). MicroRNA regulation of glycoprotein B5R in oncolytic vaccinia virus reduces viral pathogenicity without impairing its antitumor efficacy. *Mol. Ther.* *19*, 1107–1115.
- Fu, X., Rivera, A., Tao, L., De Geest, B., and Zhang, X. (2012). Construction of an oncolytic herpes simplex virus that precisely targets hepatocellular carcinoma cells. *Mol. Ther.* *20*, 339–346.
- Li, J.M., Kao, K.C., Li, L.F., Yang, T.M., Wu, C.P., Horng, Y.M., Jia, W.W., and Yang, C.T. (2013). MicroRNA-145 regulates oncolytic herpes simplex virus-1 for selective killing of human non-small cell lung cancer cells. *Virol. J.* *10*, 241.
- Ylösmäki, E., Martikainen, M., Hinkkanen, A., and Saksela, K. (2013). Attenuation of Semliki Forest virus neurovirulence by microRNA-mediated detargeting. *J. Virol.* *87*, 335–344.
- Baertsch, M.A., Leber, M.F., Bossow, S., Singh, M., Engeland, C.E., Albert, J., Grossardt, C., Jäger, D., von Kalle, C., and Ungerechts, G. (2014). MicroRNA-mediated multi-tissue detargeting of oncolytic measles virus. *Cancer Gene Ther.* *21*, 373–380.
- Bofill-De Ros, X., Gironella, M., and Fillat, C. (2014). miR-148a- and miR-216a-regulated oncolytic adenoviruses targeting pancreatic tumors attenuate tissue damage without perturbation of miRNA activity. *Mol. Ther.* *22*, 1665–1677.
- Bofill-De Ros, X., Villanueva, E., and Fillat, C. (2015). Late-phase miRNA-controlled oncolytic adenovirus for selective killing of cancer cells. *Oncotarget* *6*, 6179–6190.
- Bofill-De Ros, X., Rovira-Rigau, M., and Fillat, C. (2017). Implications of MicroRNAs in Oncolytic Virotherapy. *Front. Oncol.* *7*, 142.
- Ruiz, A.J., Hadad, E.M., Nace, R.A., and Russell, S.J. (2016). MicroRNA-Detargeted Mengovirus for Oncolytic Virotherapy. *J. Virol.* *90*, 4078–4092.
- Ruiz, A.J., and Russell, S.J. (2017). MicroRNA-based Regulation of Picornavirus Tropism. *J. Vis. Exp.* *120*, 55033.
- He, F., Yao, H., Wang, J., Xiao, Z., Xin, L., Liu, Z., Ma, X., Sun, J., Jin, Q., and Liu, Z. (2015). Coxsackievirus B3 engineered to contain microRNA targets for muscle-specific microRNAs displays attenuated cardiotoxic virulence in mice. *J. Virol.* *89*, 908–916.
- Louis, D.N., Perry, A., Reifenberger, G., von Deimling, A., Figarella-Branger, D., Cavenee, W.K., Ohgaki, H., Wiestler, O.D., Kleihues, P., and Ellison, D.W. (2016). The 2016 World Health Organization Classification of Tumors of the Central Nervous System: a summary. *Acta Neuropathol.* *131*, 803–820.
- Stupp, R., Mason, W.P., van den Bent, M.J., Weller, M., Fisher, B., Taphoorn, M.J., Belanger, K., Brandes, A.A., Marosi, C., Bogdahn, U., et al.; European Organisation for Research and Treatment of Cancer Brain Tumor and Radiotherapy Groups; National Cancer Institute of Canada Clinical Trials Group (2005). Radiotherapy plus concomitant and adjuvant temozolomide for glioblastoma. *N. Engl. J. Med.* *352*, 987–996.
- Thakkar, J.P., Dolecek, T.A., Horbinski, C., Ostrom, Q.T., Lightner, D.D., Barnholtz-Sloan, J.S., and Villano, J.L. (2014). Epidemiologic and molecular prognostic review of glioblastoma. *Cancer Epidemiol. Biomarkers Prev.* *23*, 1985–1996.
- Larkin, J., Chiarion-Sileni, V., Gonzalez, R., Grob, J.J., Cowey, C.L., Lao, C.D., Schadendorf, D., Dummer, R., Smylie, M., Rutkowski, P., et al. (2015). Combined Nivolumab and Ipilimumab or Monotherapy in Untreated Melanoma. *N. Engl. J. Med.* *373*, 23–34.
- Weller, M., Butowski, N., Tran, D.D., Recht, L.D., Lim, M., Hirte, H., Ashby, L., Mechtler, L., Goldlust, S.A., Iwamoto, F., et al.; ACT IV trial investigators (2017). Rindopepimut with temozolomide for patients with newly diagnosed, EGFRvIII-expressing glioblastoma (ACT IV): a randomised, double-blind, international phase 3 trial. *Lancet Oncol.* *18*, 1373–1385.

20. Omuro, A., Vlahovic, G., Lim, M., Sahebjam, S., Baehring, J., Cloughesy, T., Voloschin, A., Ramkissoon, S.H., Ligon, K.L., Latek, R., et al. (2018). Nivolumab with or without ipilimumab in patients with recurrent glioblastoma: results from exploratory phase I cohorts of CheckMate 143. *Neuro-oncol.* 20, 674–686.
21. Zhang, Q., and Liu, F. (2020). Advances and potential pitfalls of oncolytic viruses expressing immunomodulatory transgene therapy for malignant gliomas. *Cell Death Dis.* 11, 485.
22. Rius-Rocabert, S., García-Romero, N., García, A., Ayuso-Sacido, A., and Nistal-Villan, E. (2020). Oncolytic Virotherapy in Glioma Tumors. *Int. J. Mol. Sci.* 21, 7604.
23. McCarthy, C., Jayawardena, N., Burga, L.N., and Bostina, M. (2019). Developing Picornaviruses for Cancer Therapy. *Cancers (Basel)* 11, 685.
24. Burke, M.J., Ahern, C., Weigel, B.J., Poirier, J.T., Rudin, C.M., Chen, Y., Cripe, T.P., Bernhardt, M.B., and Blaney, S.M. (2015). Phase I trial of Seneca Valley Virus (NTX-010) in children with relapsed/refractory solid tumors: a report of the Children's Oncology Group. *Pediatr. Blood Cancer* 62, 743–750.
25. Rudin, C.M., Poirier, J.T., Senzer, N.N., Stephenson, J., Jr., Loesch, D., Burroughs, K.D., Reddy, P.S., Hann, C.L., and Hallenbeck, P.L. (2011). Phase I clinical study of Seneca Valley Virus (SVV-001), a replication-competent picornavirus, in advanced solid tumors with neuroendocrine features. *Clin. Cancer Res.* 17, 888–895.
26. Schenk, E.L., Mandrekar, S.J., Dy, G.K., Aubry, M.C., Tan, A.D., Dakhil, S.R., Sachs, B.A., Nieva, J.J., Bertino, E., Lee Hann, C., et al. (2020). A Randomized Double-Blind Phase II Study of the Seneca Valley Virus (NTX-010) versus Placebo for Patients with Extensive-Stage SCLC (ES SCLC) Who Were Stable or Responding after at Least Four Cycles of Platinum-Based Chemotherapy: North Central Cancer Treatment Group (Alliance) N0923 Study. *J. Thorac. Oncol.* 15, 110–119.
27. Zimmerman, J. (1994). Encephalomyocarditis. In *CRC Handbook Series in Zoonoses*, 2nd edition, G.W. Beran, ed. (CRC Press), pp. 423–436.
28. Thomson, G.R., Bengis, R.G., and Brown, C.C. (2001). Picornavirus Infections. In *Infectious Diseases of Wild Mammals*, Third Edition, E.S. Williams and I.K. Barker, eds. (Wiley).
29. Backues, K.A., Hill, M., Palmenberg, A.C., Miller, C., Soike, K.F., and Aguilar, R. (1999). Genetically engineered Mengo virus vaccination of multiple captive wildlife species. *J. Wildl. Dis.* 35, 384–387.
30. Osorio, J.E., Hubbard, G.B., Soike, K.F., Girard, M., van der Werf, S., Moulin, J.C., and Palmenberg, A.C. (1996). Protection of non-murine mammals against encephalomyocarditis virus using a genetically engineered Mengo virus. *Vaccine* 14, 155–161.
31. Osorio, J.E., Martin, L.R., and Palmenberg, A.C. (1996). The immunogenic and pathogenic potential of short poly(C) tract Mengo viruses. *Virology* 223, 344–350.
32. Xia, H., Cheung, W.K.C., Ng, S.S., Jiang, X., Jiang, S., Sze, J., Leung, G.K.K., Lu, G., Chan, D.T.M., Bian, X.W., et al. (2012). Loss of brain-enriched miR-124 microRNA enhances stem-like traits and invasiveness of glioma cells. *J. Biol. Chem.* 287, 9962–9971.
33. Romanova, L.I., Lidsky, P.V., Kolesnikova, M.S., Fominykh, K.V., Gmyl, A.P., Sheval, E.V., Hato, S.V., van Kuppeveld, F.J.M., and Agol, V.I. (2009). Antiapoptotic activity of the cardiovirus leader protein, a viral “security” protein. *J. Virol.* 83, 7273–7284.
34. Hato, S.V., Ricour, C., Schulte, B.M., Lanke, K.H.W., de Bruijini, M., Zoll, J., Melchers, W.J.G., Michiels, T., and van Kuppeveld, F.J.M. (2007). The mengovirus leader protein blocks interferon- $\alpha$ /beta gene transcription and inhibits activation of interferon regulatory factor 3. *Cell. Microbiol.* 9, 2921–2930.
35. Borghese, F., and Michiels, T. (2011). The leader protein of cardioviruses inhibits stress granule assembly. *J. Virol.* 85, 9614–9622.
36. Pelletier, M., and Montplaisir, S. (1975). The nude mouse: a model of deficient T-cell function. *Methods Achiev. Exp. Pathol.* 7, 149–166.
37. Zoll, J., Melchers, W.J., Galama, J.M., and van Kuppeveld, F.J. (2002). The mengovirus leader protein suppresses alpha/beta interferon production by inhibition of the iron/ferritin-mediated activation of NF- $\kappa$ B. *J. Virol.* 76, 9664–9672.
38. Paul, S., and Michiels, T. (2006). Cardiovirus leader proteins are functionally interchangeable and have evolved to adapt to virus replication fitness. *J. Gen. Virol.* 87, 1237–1246.
39. Chinsangaram, J., Piccone, M.E., and Grubman, M.J. (1999). Ability of foot-and-mouth disease virus to form plaques in cell culture is associated with suppression of alpha/beta interferon. *J. Virol.* 73, 9891–9898.
40. Fan, J., Son, K.N., Arslan, S.Y., Liang, Z., and Lipton, H.L. (2009). Theiler's murine encephalomyelitis virus leader protein is the only nonstructural protein tested that induces apoptosis when transfected into mammalian cells. *J. Virol.* 83, 6546–6553.
41. Metz, G.E., Abeyá, M.M., Serena, M.S., Panei, C.J., and Echeverría, M.G. (2019). Evaluation of apoptosis markers in different cell lines infected with equine arteritis virus. *Biotech. Histochem.* 94, 115–125.
42. Cerami, E., Demir, E., Schultz, N., Taylor, B.S., and Sander, C. (2010). Automated network analysis identifies core pathways in glioblastoma. *PLoS ONE* 5, e8918.
43. Pomykala, H.M., Bohlander, S.K., Broecker, P.L., Olopade, O.I., and Díaz, M.O. (1994). Breakpoint junctions of chromosome 9p deletions in two human glioma cell lines. *Mol. Cell. Biol.* 14, 7604–7610.
44. Lin, A.H., Burrascano, C., Pettersson, P.L., Ibañez, C.E., Gruber, H.E., and Jolly, D.J. (2014). Blockade of type I interferon (IFN) production by retroviral replicating vectors and reduced tumor cell responses to IFN likely contribute to tumor selectivity. *J. Virol.* 88, 10066–10077.
45. Ano, Y., Sakudo, A., and Onodera, T. (2012). Role of microglia in oxidative toxicity associated with encephalomyocarditis virus infection in the central nervous system. *Int. J. Mol. Sci.* 13, 7365–7374.
46. Russell, S.J., Peng, K.W., and Bell, J.C. (2012). Oncolytic virotherapy. *Nat. Biotechnol.* 30, 658–670.
47. Suryawanshi, Y.R., Zhang, T., and Essani, K. (2017). Oncolytic viruses: emerging options for the treatment of breast cancer. *Med. Oncol.* 34, 43.
48. Pol, J., Buqué, A., Aranda, F., Bloy, N., Cremer, I., Eggermont, A., Erbs, P., Fucikova, J., Galon, J., Limacher, J.M., et al. (2015). Trial Watch-Oncolytic viruses and cancer therapy. *Oncoimmunology* 5, e1117740.
49. Pol, J.G., Lévesque, S., Workenhe, S.T., Gujar, S., Le Boeuf, F., Clements, D.R., Fahrner, J.E., Fend, L., Bell, J.C., Mossman, K.L., et al. (2018). Trial Watch: Oncolytic viro-immunotherapy of hematologic and solid tumors. *Oncoimmunology* 7, e1503032.
50. Kelly, E.J., Hadac, E.M., Cullen, B.R., and Russell, S.J. (2010). MicroRNA antagonism of the picornaviral life cycle: alternative mechanisms of interference. *PLoS Pathog.* 6, e1000820.
51. Kelly, E.J., Hadac, E.M., Greiner, S., and Russell, S.J. (2008). Engineering microRNA responsiveness to decrease virus pathogenicity. *Nat. Med.* 14, 1278–1283.
52. Barnes, D., Kunitomi, M., Vignuzzi, M., Saksela, K., and Andino, R. (2008). Harnessing endogenous miRNAs to control virus tissue tropism as a strategy for developing attenuated virus vaccines. *Cell Host Microbe* 4, 239–248.
53. Buijs, P.R., Verhagen, J.H., van Eijck, C.H., and van den Hoogen, B.G. (2015). Oncolytic viruses: From bench to bedside with a focus on safety. *Hum. Vaccin. Immunother.* 11, 1573–1584.
54. Carocci, M., Cordonnier, N., Huet, H., Romey, A., Relmy, A., Gorna, K., Blaise-Boisseau, S., Zientara, S., and Kassimi, L.B. (2011). Encephalomyocarditis virus 2A protein is required for viral pathogenesis and inhibition of apoptosis. *J. Virol.* 85, 10741–10754.
55. Stojdl, D.F., Lichty, B., Knowles, S., Marius, R., Atkins, H., Sonenberg, N., and Bell, J.C. (2000). Exploiting tumor-specific defects in the interferon pathway with a previously unknown oncolytic virus. *Nat. Med.* 6, 821–825.
56. Matveeva, O.V., and Chumakov, P.M. (2018). Defects in interferon pathways as potential biomarkers of sensitivity to oncolytic viruses. *Rev. Med. Virol.* 28, e2008.
57. Mishima, T., Mizuguchi, Y., Kawahigashi, Y., Takizawa, T., and Takizawa, T. (2007). RT-PCR-based analysis of microRNA (miR-1 and -124) expression in mouse CNS. *Brain Res.* 1131, 37–43.
58. Yao, L., Ye, Y., Mao, H., Lu, F., He, X., Lu, G., and Zhang, S. (2018). MicroRNA-124 regulates the expression of MEK3 in the inflammatory pathogenesis of Parkinson's disease. *J. Neuroinflammation* 15, 13.
59. Blasi, E., Barluzzi, R., Bocchini, V., Mazzolla, R., and Bistoni, F. (1990). Immortalization of murine microglial cells by a v-raf/v-myc carrying retrovirus. *J. Neuroimmunol.* 27, 229–237.
60. Righi, M., Mori, L., De Libero, G., Sironi, M., Biondi, A., Mantovani, A., Donini, S.D., and Ricciardi-Castagnoli, P. (1989). Monokine production by microglial cell clones. *Eur. J. Immunol.* 19, 1443–1448.

61. Das, A., Kim, S.H., Arifuzzaman, S., Yoon, T., Chai, J.C., Lee, Y.S., Park, K.S., Jung, K.H., and Chai, Y.G. (2016). Transcriptome sequencing reveals that LPS-triggered transcriptional responses in established microglia BV2 cell lines are poorly representative of primary microglia. *J. Neuroinflammation* *13*, 182.
62. Aw, E., Zhang, Y., and Carroll, M. (2020). Microglial responses to peripheral type I interferon. *J. Neuroinflammation* *17*, 340.
63. Stern, A., Bianco, S., Yeh, M.T., Wright, C., Butcher, K., Tang, C., Nielsen, R., and Andino, R. (2014). Costs and benefits of mutational robustness in RNA viruses. *Cell Rep.* *8*, 1026–1036.
64. Tardieu, M., Powers, M.L., and Weiner, H.L. (1983). Age dependent susceptibility to Reovirus type 3 encephalitis: role of viral and host factors. *Ann. Neurol.* *13*, 602–607.
65. Coffey, M.C., Strong, J.E., Forsyth, P.A., and Lee, P.W. (1998). Reovirus therapy of tumors with activated Ras pathway. *Science* *282*, 1332–1334.
66. Mader, E.K., Maeyama, Y., Lin, Y., Butler, G.W., Russell, H.M., Galanis, E., Russell, S.J., Dietz, A.B., and Peng, K.W. (2009). Mesenchymal stem cell carriers protect oncolytic measles viruses from antibody neutralization in an orthotopic ovarian cancer therapy model. *Clin. Cancer Res.* *15*, 7246–7255.
67. Wynne, A.M., Henry, C.J., Huang, Y., Cleland, A., and Godbout, J.P. (2010). Protracted downregulation of CX3CR1 on microglia of aged mice after lipopolysaccharide challenge. *Brain Behav. Immun.* *24*, 1190–1201.
68. Jankov, I.D., Penheiter, A.R., Griesmann, G.E., Carlson, S.K., Federspiel, M.J., and Galanis, E. (2013). Neutralization capacity of measles virus H protein specific IgG determines the balance between antibody-enhanced infectivity and protection in microglial cells. *Virus Res.* *172*, 15–23.
69. Fata-Hartley, C.L., and Palmenberg, A.C. (2005). Dipyridamole reversibly inhibits mengovirus RNA replication. *J. Virol.* *79*, 11062–11070.
70. Bochkov, Y.A., and Palmenberg, A.C. (2006). Translational efficiency of EMCV IRES in bicistronic vectors is dependent upon IRES sequence and gene location. *Biotechniques* *41*, 283–284, 286, 288 passim.